Final Report

Project Title: THERMOCHEMISTRY AND REACTIVITY OF METALS ENGAGED IN CHEMIIONIZATION

Institution:	University of Utah, Department of Chemistry
Street Address:	315 South 1400 East, Room 2020 Salt Lake City, UT 84112-0850
Principal Investigator:	Peter B. Armentrout
Address:	Department of Chemistry University of Utah 315 South 1400 East, Room 2020 Salt Lake City, UT 84112-0850
Telephone Number:	(801) 581-7885
Email:	armentrout@chem.utah.edu

Funding Opportunity Announcement Number: BAA-AFOSR-2014-0001

CFDA 12.800 CID RTE-4

Air Force Office of Scientific Research
Energy, Power and Propulsion Sciences (RTE)
Molecular Dynamics and Theoretical Chemistry (RTE-4)

Program Officer: : Dr. Michael R. Berman AFOSR/RTE (703) 696-7781
DSN 426-7781; FAX (703) 696-7320
E-mail: **michael.berman@us.af.mil**

AFOSR Grant Number: FA9550-14-1-0357

THERMOCHEMISTRY AND REACTIVITY OF METALS ENGAGED IN CHEMIIONIZATION

Principal Investigator: Peter B. Armentrout (armentrout@chem.utah.edu)
Institution: University of Utah, Department of Chemistry
Salt Lake City, UT 84112-0850

Funding Opportunity Announcement Number: BAA-AFOSR-2014-0001; CFDA 12.800

Air Force Office of Scientific Research; Energy, Power and Propulsion Sciences (RTE)
Molecular Dynamics and Theoretical Chemistry (RTE-4)

Program Officer: : Dr. Michael R. Berman AFOSR/RTE (**michael.berman@us.af.mil**)

I. Statement of Objectives

The thermochemistry and reactivity of oxidation reactions of lanthanides have implications for understanding chemiionization reactions of these elemental metals. The Air Force has explored the possibility of using the chemiionization reactions of atomic metal ions with oxygen atoms available in the ionosphere as a means to form enhanced plasma densities in the atmosphere. Such man-made plasmas are one potential means to mitigate scintillation effects that interfere with satellite communications. Underscoring the need for fundamental information regarding such reactions are recent atmospheric release studies involving samarium metal, which failed to proceed as expected. To understand this failure, it became clear that the literature data regarding the thermodynamics, reactivity, and dynamics of samarium oxidation was incomplete.

To acquire thermodynamic information on the oxidation of samarium and other lanthanides, reactions of the atomic metal cations and their oxides with atmospheric gases (O_2, CO, CO_2, NO, H_2O) will be studied as a function of kinetic energy in a guided ion beam tandem mass spectrometer (GIBMS). Such reactions are of direct interest in understanding the chemistry that might occur when such lanthanides are exposed to atmospheric air at high temperature. Analysis of such data will provide quantitative bond energies of a variety of species yielding a better fundamental understanding of their chemical and physical properties. Such thermodynamic data will also provide better predictability regarding the reactivity of lanthanides, which is then augmented by the direct kinetic data obtained for the specific reactions examined. Both the kinetic and thermodynamic data will be useful in modeling the chemistry of these species.

Accurate quantum chemical calculations on heavy metal species are particularly problematic because of the need to implement relativistic quantum chemistry under conditions in which electron correlation is also of great importance. The challenges of these calculations are exacerbated by a shortage of accurate information on such heavy metal molecules, which makes validation of the approximations employed difficult. One aim of the present work was to develop a base of accurate thermochemical data, thereby providing benchmarks against which quantum chemical methods may be tested.

Accompanying its scientific merit is the fact that this work involved the education of graduate and undergraduate students in lanthanide science and experiments.

II. Research Effort

A. Background

Satellite communications (e.g., global positioning systems, GPS, and telecommuncations) are of clear importance in both the civilian and military sectors, however, scintillation effects can interfere with radio wave propagation leading to intermittent or complete loss of communication. Scintillation can be caused by natural irregularities in the ionosphere. In critical applications, it may be desirable to mitigate these scintillation effects by directly inducing man-made enhanced plasma densities to slow the growth of the ionospheric instabilities. The Air Force has explored the possibility of creating such artificial plasma clouds by increasing the electron density using chemical release. Materials such as barium, strontium, xenon, lithium, and cesium have been studied, but require solar photons or particle collisions for ionization, hence limiting their efficiency. Other processes that hold higher promise in this regard are chemiionization processes, and in particular, reaction 1 where M is an elemental metal.

$$M + O \rightarrow MO^+ + e^- \qquad \Delta H < 0 \text{ kJ/mol} \qquad (1)$$

If reaction 1 is exothermic, this process can occur spontaneously by utilizing the atomic oxygen present at the altitudes of interest. Further, the undesirable reverse reaction is inefficient because it is endothermic. (This simplistic conclusion is mediated by the fact that the electron temperature in the ionosphere is ~1000 K, such that some appreciable fraction of energetic electrons can undergo the reverse reaction if reaction 1 is not exothermic by more than ~0.4 eV.) Recently, Air Force Research Laboratory (AFRL) Metal Oxide Space Cloud (MOSC) experiments have been conducted to test the efficiency of forming an artificial plasma cloud by this process using samarium, M = Sm. Samarium was chosen for these initial experiments because the literature thermochemistry indicated the reaction was exothermic by about 0.3 eV,[1] and samarium has a relatively low boiling point (2067 K), which would allow efficient vaporization of this material using a titanium-boron thermite mixture that reaches temperatures of about 3500 K. Predictions of the test suggested that only a few kg of metal dispersed in the ionosphere near an altitude of 170 km could create an enhanced plasma cloud over distances extending as far as 100 km. Unfortunately, the plasma density produced was about two orders of magnitude smaller than expected, and the cloud shape and color all differed significantly from pre-launch predictions.

To understand these phenomena, the plasma chemistry research group of Dr. Albert Viggiano at AFRL was contacted to explore the chemistry of samarium more thoroughly. Using their selected ion flow tube (SIFT) apparatus equipped with an electrospray ionization (ESI) source, they determined the rates and temperature dependences of several reactions of Sm^+ and SmO^+ near room temperature, finding that N_2O, NO_2, O_2, and SO_2 all react with Sm^+ to form SmO^+.[2] Examination of the thermochemistry in Table 1 shows that these observations suggest that $D(Sm^+\text{-}O) > 5.66$ eV = D(OS-O). In contrast, the SIFT studies also found that CO_2 and NO were unreactive with Sm^+. Because D(OC-O) is lower than 5.66 eV (Table 1), the failure to react with CO_2 at room temperature cannot be a consequence of unfavorable thermodynamics, but rather must result from kinetic effects. In addition, the SIFT studies determined that SmO^+ reacted with N_2O, NO_2, O_2, CO_2, SO_2, and NO exclusively by three-body association.

Table 1
Oxide Bond Energies

Species	D_0(M-O), eV
N_2O	1.672 ± 0.004
NO_2	3.116 ± 0.009
H_2O	5.034 ± 0.001
O_2	5.115 ± 0.001
CO_2	5.453 ± 0.002
SO_2	5.66 ± 0.02
NO	6.507 ± 0.002
CO	11.108 ± 0.005

Unfortunately, these data yielded no specific insight into the MOSC results, hence, the PIs laboratory was contacted to see if we could elucidate the thermochemistry of SmO and SmO^+ more thoroughly.

As described further below, the guided ion beam tandem mass spectrometry (GIBMS) approach developed in the PIs laboratory has proven to be a versatile experimental method of determining quantitative thermodynamic information. In this particular case, the PI and his graduate student, Richard M Cox, studied several reactions that provided specific information regarding the bond energy of SmO^+, with the results having recently been published.[2] These data indicate a substantially lower bond energy than suggested in the literature, sufficiently so that reaction 1 now appears to be exothermic by only 0.08 ± 0.07 eV. Simulations of the MOSC test using this thermodynamic information are in agreement with the experimental results from this test, thereby confirming the utility of the fundamental thermodynamic data provided by the PIs laboratory. Continued work on these systems has extended our results to that of gadolinium oxide (Gd), as studied by graduate student, Maria Demireva.

B. Experimental methods

Overview. The experimental technique we use is GIBMS.[3] This device uses mass spectrometry to select an ionic reactant, which reacts under single collision conditions with neutral molecules in a radiofrequency (rf) octopole ion beam guide, and then analyzes the products using mass spectrometry, with single molecule sensitivity. The Utah GIBMS instrument allows the study of the kinetic energy dependence of ion-molecule reactions over a wide (four order of magnitude) energy range. This enables the measurement of the thermodynamics of metal-ligand interactions using two types of processes: exchange reactions 2,

$$M^+ + LR \rightarrow ML^+ + R \qquad (2)$$

and collision-induced dissociation (CID), reactions 3.

$$ML_x^+ + Xe \rightarrow ML_{x-1}^+ + L + Xe \qquad (3)$$

In the first case, if the reaction is endothermic, the threshold for reaction, E_0, can be measured and related to the bond dissociation energy (BDE) of M^+-L by $D_0(M^+\text{-}L) = D_0(LR) - E_0$, where $D_0(LR)$ is taken from the literature. In the CID process, which is intrinsically endothermic, E_0 equals $D_0(L_{x-1}M^+\text{-}L)$ as long as there are no barriers to the reverse process, which is generally the case because of the long-range attractive character of ions with polarizable and polar molecules.[4] Accurate determination of metal-ligand BDEs using this approach requires that several factors be taken into account, as detailed below.[5-6]

Ion generation. The ion source is a critical feature for the quantitative study of the energetics of ion-molecule reactions. Unless the internal energy of the ions is adequately controlled, our knowledge of the energy available to reaction and thus the precision and accuracy of any thermodynamic measurement is compromised. For the studies proposed here, this control is achieved using a dc discharge/flow tube (DC/FT) source.[7-13] This source has been used to generate atomic metal and metal oxide ions for studies of reactions 2 and 3 with most of the transition metals (TMs), measuring a wide variety of covalent metal-ligand bonds.[14-15] It is also the source used in the samarium and preliminary gadolinium chemistry outlined below, as well as recent work on the actinide thorium.[16] In this source, argon (about 10% in He) is ionized by a kV dc potential and then collides with the cathode composed of or containing the material of interest, essentially sputtering the desired metal cations. Ions generated in this glow discharge can then undergo further reaction (such as oxidation or condensation) in the meter-long flow

tube. In addition, the ions are thermalized by undergoing about 10^5 collisions with the inert flow gases. For atomic transition metal cations, we have demonstrated that the distribution of electronic states produced by the DC/FT source is thermal or nearly so. For instance, by comparing results with those from a surface ionization source (where the source temperature is known), the DC/FT source has been found to generate Sc^+,[17] Fe^+,[18] Co^+,[19] Ni^+,[20] Ru^+,[21] Rh^+,[21] and Pd^+ [21] ions with an average electronic temperature of 700 ± 400 K, and Y^+, Zr^+, Nb^+, and Mo^+ ions with an average electronic temperature of 300 ± 100 K.[22] Therefore, we conservatively quote the DC/FT source temperature as 700 ± 400 K. For lanthanide cations, this means that the dominant species occupied is the ground state term.

As detailed below, the DC/FT source can produce species such as M^+, MO^+, and MO_2^+ for M = Sm and Gd. We have also demonstrated that termolecular reactions can attach one or many ligands of all sorts (Ar, CO, N_2, H_2O, CO_2, amino acids, through crown ethers) to bare metal and oxygenated ions throughout the periodic table,[8-9,11,13,23-25] thereby generating a wide range of ML_x^+ species, e.g., $M^+(O_2)$, $M^+(CO_2)$ and $OM^+(CO)$. Using reactions 3, quantitative measurements of noncovalent metal-ligand interactions have been examined for alkalis, alkaline earth, and transition metal ions with a wide range of ligands.[14-15,25] Below, such studies are illustrated by determination of the bond energies of Sm^+–CO_2, OSm^+-CO, and $Gd^+(O_2)$.

Guided ion beam mass spectrometry. Once the ions leave the source, they pass through a differentially pumped chamber where they are focused into a beam and mass analyzed. They then enter another chamber, where they are decelerated to a desired kinetic energy and injected into an rf octopole beam guide,[26] which acts as a radial ion trap. The octopole passes through a reaction cell containing a neutral reactant gas maintained at sufficiently low pressure that single-collision conditions prevail. The pressure dependence of all cross sections is measured to ensure that rigorous single-collision conditions are used in the data analysis. Product and remaining reactant ions drift to the end of the octopole, where they are focused into a final differentially pumped chamber. (In one instrument, the octopole region contains two octopoles, which allows additional dynamics experiments to be conducted.[27]) Here, the ions are separated with a quadrupole mass filter and detected using a secondary electron scintillation (Daly) detector[28] and standard ion pulse counting techniques that provide essentially unit detection capability up to high masses. Data collection is under computer control, which allows extensive signal averaging. At each relative kinetic energy, E, the intensities of transmitted reactant and product ions are converted to absolute reaction cross sections for each product channel, $\sigma(E)$.[3] These cross sections have absolute uncertainties of ±20%. Relative cross sections are accurate to about ±5%.

There are several advantages to using guided ion beam techniques to study ion-molecule reactions. First, the range of energies available to the instrument is extensive, four orders of magnitude ranging from thermal to a thousand electron volts. This is the primary distinction between this method of examining gas-phase ion-molecule chemistry and other instrumentation, which is generally limited to thermal energies. Second, the absolute kinetic energy scale can be determined accurately using the octopole as a highly efficient retarding energy analyzer. Third, the octopole ion beam guide allows for highly efficient product collection.[3,27,29] Fourth, because the octopole extends well beyond the ends of the gas cell (unlike triple quadrupole collision regions), the collision energy is well-controlled and the $1/r^6$ effective potential is much less perturbing than the $1/r^2$ potential in quadrupoles.

Data analysis. The ability to examine reactions over a very wide range of kinetic energies is the distinguishing and truly powerful ability of guided ion beam methods. This capability allows endothermic reactions to be examined routinely. By measuring the threshold

for reaction, we can obtain thermodynamic information on the reaction products for a wide variety of species. This generally assumes that activation barriers in excess of the endothermicity are not present. This assumption is generally valid for ion-molecule reactions, largely because of the long-range attractive form of ion-molecule interactions,[30] as long as there are no constraints resulting from spin or orbital angular momentum conservation.[5] (Interestingly, the samarium chemistry provides a couple of examples where such unusual constraints are evident, although not yet completely understood, as discussed further below.) For CID studies involving heterolytic bond cleavages, which encompasses many of the systems of interest here, we have shown that there should be no reverse activation barriers because of electronic considerations.[4]

Our methods of analysis have been amply described in the literature,[5-6] and have proven to be robust for a large number of species. Briefly, we use Eq. 4 to reproduce the energy dependence of reaction cross sections.

$$\sigma(E) = \left(\frac{n\sigma_o}{E}\right)\sum_i g_i \int_{E_o - E_i}^{E} (1 - e^{-k(\varepsilon + E_i)\tau})(E - \varepsilon)^{n-1} d\varepsilon \qquad (4)$$

Here, σ_0 is an energy independent scaling factor, E is the relative translational energy of the ion, E_0 is the reaction threshold at 0 K, and n is an adjustable fitting parameter that describes the efficiency of the energy transfer upon collision.[27] The summation is over the rovibrational and electronic states of the reactants having excitation energies, E_i, and populations, g_i, where $\Sigma g_i = 1$. ε represents the energy deposited into the ion upon collision with the neutral reagent, and τ is the average timescale of the experiment (ion time-of-flight from the collision cell to the quadrupole mass spectrometer, either ~0.1 or 0.5 ms for the single and dual octopole instruments, respectively). The rate constant, $k(\varepsilon + E_i) = k(E^*)$, is the Rice-Ramsperger-Kassel-Marcus (RRKM) unimolecular dissociation rate constant[31-32] as calculated using Eq. 5,

$$k(E^*) = sN^{\dagger}_{vr}(E^* - E_0) / h\rho_{vr}(E^*) \qquad (5)$$

where s is the reaction degeneracy calculated from the ratio of rotational symmetry numbers of the reactants with respect to the products, $N^{\dagger}_{vr}(E^* - E_0)$ is the sum of the rovibrational states of the transition state (TS) at an energy $E^* - E_0$ above the threshold, E_0, and $\rho_{vr}(E^*)$ is the density of rovibrational states for the energized molecule (EM) at the energy available, E^*. When the rate constant is much faster than the average experimental timescale (which is generally true for small molecular systems), Eq. 4 reduces to Eq. 6,

$$\sigma(E) = \sigma_0 \sum g_i (E + E_i - E_0)^n / E \qquad (6)$$

a simple modified line-of-centers form. This form is often sufficient to analyze the cross sections for exchange reactions 2. After convolution over the kinetic energy distributions of both reactants, Eqs. 4 and 6 have been shown to accurately describe the kinetic energy dependence of many bimolecular reactions and CID experiments (see examples below in Figures 2 and 3).

This model for the kinetic energy dependence of ion-molecule reactions includes explicit consideration of the internal energy of both reactants,[3,33-35] and has been shown to be directly compatible with direct measurements of the energy transfer function.[27] For CID of larger systems, the model includes the possibility that the collisionally excited complex does not dissociate during the experimental flight time, which can lead to a delayed onset for the CID threshold, a kinetic shift. Our model includes an estimate of this effect by incorporating statistical rate theory for the unimolecular rate of dissociation of an energized molecule.[36-37] Several reasonable treatments of the assumed energy and angular momentum distributions of the

collisionally activated molecules were considered. This statistical approach also allows a straightforward introduction of competing dissociation channels,[38] for which results demonstrate that a statistical model for the rotational energy distributions gives the most accurate thermodynamic data. Additional work shows that the best results may require explicit handling of internal rotations.[39] These statistical analysis methods have been extensively tested and further developed.[40-45] These studies demonstrate that a phase space theory (PST) approach in which rotational and orbital angular momentum are explicitly conserved and allowed to interchange provides the best reproduction of the data, however, they also demonstrate that the thermodynamic information obtained is insensitive to the assumptions regarding angular momentum. Overall, the model has been shown to reproduce the threshold regions of a variety of endothermic ion-molecule reactions, including CID, with good accuracy in the resulting thermochemistry. Recent efforts have now extended our "toolbox" of thermodynamic methodology from simple bimolecular reactions and CID, to variants involving competitive[38] and sequential dissociation pathways,[46] as well as to association[44] and ligand exchange reactions.[45] These methods therefore allow multiple pathways for obtaining and verifying accurate bond energies, as well as free energies and entropies. Although the precision of such measurements does not approach spectroscopic analogues, it is nevertheless still quite good, often less than 0.1 eV and occasionally as low as 0.02 eV.[47]

C. Results

Reactions involving samarium. The literature regarding the BDE of SmO, D_0(SmO), has been reviewed thoroughly in our recent paper.[2] Data from several high temperature studies yield BDEs with a range of 5.5 ± 0.2 – 6.10 ± 0.03 eV[48-50] and have been analyzed in several compilations.[51-55] The most inclusive and conservative value is 5.88 ± 0.17 eV.[52] The ionization energy of SmO, IE(SmO), has been measured using electron ionization and high temperature mass spectrometry as 5.55 ± 0.1 eV.[56] These two pieces of information alone allow the enthalpy of reaction 1, $\Delta H_0(1)$ = IE(MO) - D_0(MO), to be determined as 5.55 – 5.88 = -0.33 ± 0.20 eV. Combined with IE(Sm) = 5.6437 eV,[57] these data also indicate that the BDE of SmO^+, $D_0(Sm^+–O)$, equals 5.97 ± 0.20 eV because IE(MO) - D_0(MO) = IE(M) - $D_0(MO^+)$. This BDE is consistent with the observations of the AFRL laboratory using their SIFT apparatus that reaction of Sm^+ with N_2O, NO_2, O_2, and SO_2 were all exothermic to form SmO^+, as well as the lack of reaction with NO as it is endothermic (Table 1).[2] This BDE also indicates that reaction with CO_2 is exothermic, whereas no reactivity was observed at thermal energies between Sm^+ and CO_2 in the AFRL SIFT studies.[2]

In our GIBMS studies of the reactions of Sm^+, the ions were generated using the DC/FT source. For Sm^+, an electronic temperature of 700 ± 400 K means that 21 – 68 % of the ions are in their ground $^8F_{1/2}$ level with 27 – 34% in the $^8F_{3/2}$ level at 0.04 eV, and 4 – 21% in the $^8F_{5/2}$ level at 0.104 eV.[58] Overall, the average electronic energy is 0.06 ± 0.05 eV, an uncertainty that is included in our determination of the threshold energies.

Our results for reaction of Sm^+ with O_2, SO_2, CO_2, and NO agree with the AFRL findings and are shown in Figure 1. Figures 1a and 1b show that the reactions of Sm^+ with O_2 and SO_2 efficiently form SmO^+ with cross sections exhibiting no barrier as low in energy as we can go, suggesting that $D_0(SmO^+) > D_0(O_2)$ = 5.115 eV and $D_0(SmO^+) > D_0$(OS-O) = 5.66 eV. In the O_2 system, the cross section matches the predicted Langevin-Gioumousis-Stevenson (LGS) collision cross section for ion-molecule reactions,[30] suggesting a reaction efficiency of 100 ± 20%. This efficiency differs from the AFRL SIFT result of about 50%, which agrees with a previous

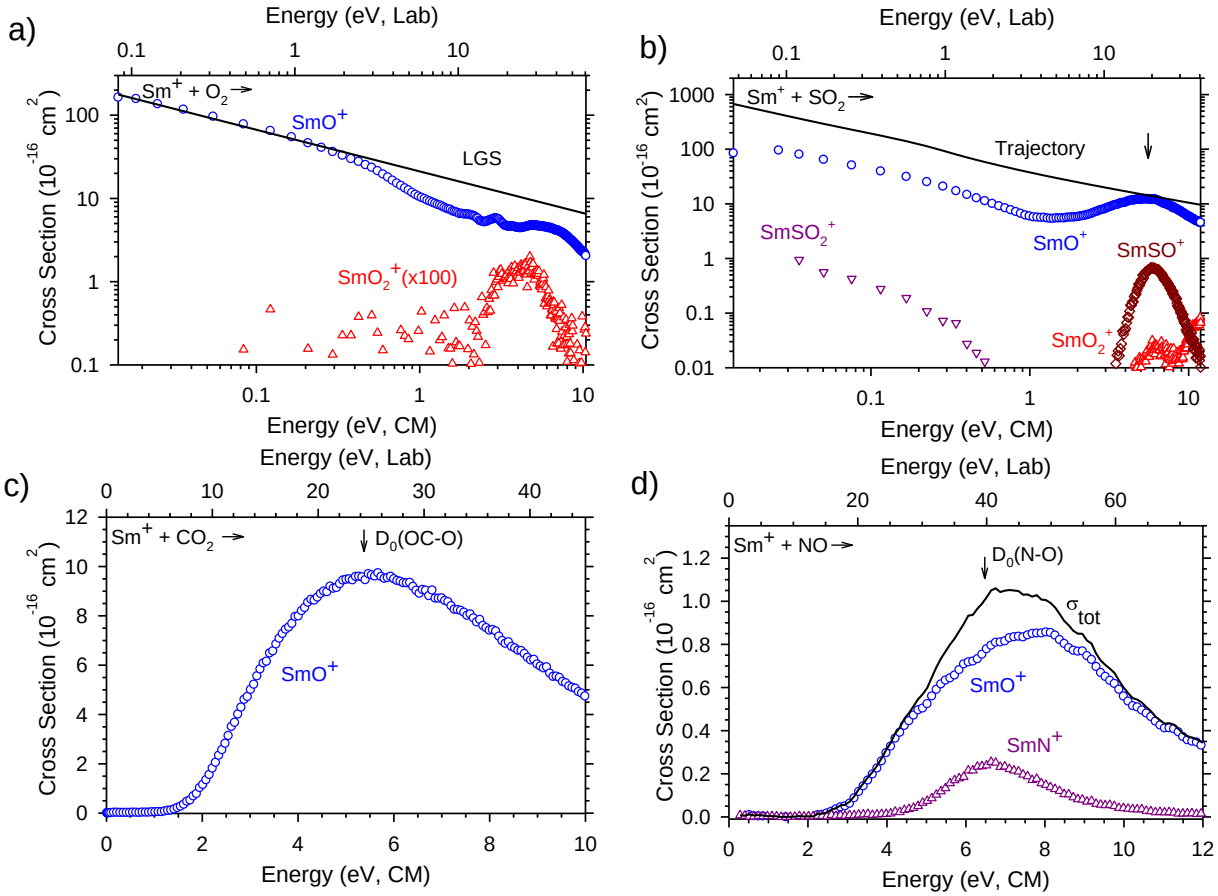

Fig. 1. Cross sections for reaction of Sm^+ with O_2, SO_2, CO_2, and NO as a function of kinetic energy in the center-of-mass (lower axis) and laboratory (upper axis) frames. Arrows indicate the bond energies of the neutral reactants. Oscillations in the cross section for SmO^+ in parts a and d are artifacts of the ion focusing. The SmO_2^+ product in part a shows a linear dependence on the pressure of O_2.

literature report (also SIFT work),[59] a discrepancy that is not understood although it could be related to the different ion sources used. For the SO_2 reaction, the SmO^+ cross section parallels the collision cross section (calculated here using the Su-Chesnavich semi-classical trajectory method to account for the dipole of SO_2)[60] at low energies and has an efficiency of 22 ± 4%, similar to the SIFT results, 29 ± 9%.

In the O_2 system, the SmO_2^+ product is observed at higher energies, but this cross section depends linearly on the O_2 pressure indicating that it is formed by reaction of the SmO^+ product with another molecule of O_2. In the SO_2 system, several minor products are observed. Figures 1c and 1d clearly show that the reactions of Sm^+ with CO_2 and NO exhibit barriers (a similar result is also obtained for oxidation of Sm^+ by OCS), consistent with the failure to observe any reaction at thermal energies in the SIFT studies. Our analysis of these cross sections using the methods discussed above yield thresholds for these reactions of 1.84 ± 0.12 eV and 2.59 ± 0.16 eV, respectively. If these thresholds corresponded to the asymptotic energies of the products, they could be combined with the CO_2 and NO bond energies, Table 1, to yield $D_0(Sm^+–O)$ = 3.61 ± 0.12 and 3.92 ± 0.17 eV, respectively. These values cannot correspond to the true BDE otherwise the oxidation of Sm^+ by O_2 and SO_2 would be endothermic. Thus, these thresholds must actually correspond to barriers along the potential energy surfaces, a result that can be explicitly demonstrated by examining the reverse reaction, as discussed further below. *These barriers are actually fairly unusual in ion-molecule chemistry and continue to be explored. Their elucidation should reveal interesting electronic properties of lanthanide chemistry.*

We also examined several reactions not previously studied by the AFRL group, including $Sm^+ + CO$, $SmO^+ + Xe$, and $SmO^+ + O_2$. Our results for these processes are shown in Figure 2, where the modeling of the data is also shown. (Reaction of $SmO^+ + O_2$ also forms SmO_2^+ in an endothermic process that allows $D_0(OSm^+\text{-}O) = 1.14 \pm 0.15$ eV to be measured.[2]) For reaction with CO, the threshold for SmO^+ production is 5.49 ± 0.12 eV, which combined with $D_0(CO)$ in Table 1, yields $D_0(SmO^+) = 5.62 \pm 0.15$ eV, which is consistent with the exothermic reaction of $Sm^+ + O_2$ and SO_2 within experimental uncertainty. In the collision-induced dissociation (CID) reactions with Xe and O_2, the thresholds measured are 5.67 ± 0.16 and 5.78 ± 0.09 eV, respectively. These values should directly correspond to $D_0(SmO^+)$, although conservatively they are upper limits as the translational to internal energy transfer can be inefficient for strongly bound species like SmO^+. Notably, these three BDEs are within experimental uncertainty of each other and have a weighted average of $D_0(Sm^+\text{-}O) = 5.72_5 \pm 0.07$ eV (one standard deviation).[2] This value also agrees with the best literature value, 5.97 ± 0.20 eV, within combined experimental uncertainties, but is more precise and lower by 0.25 eV.

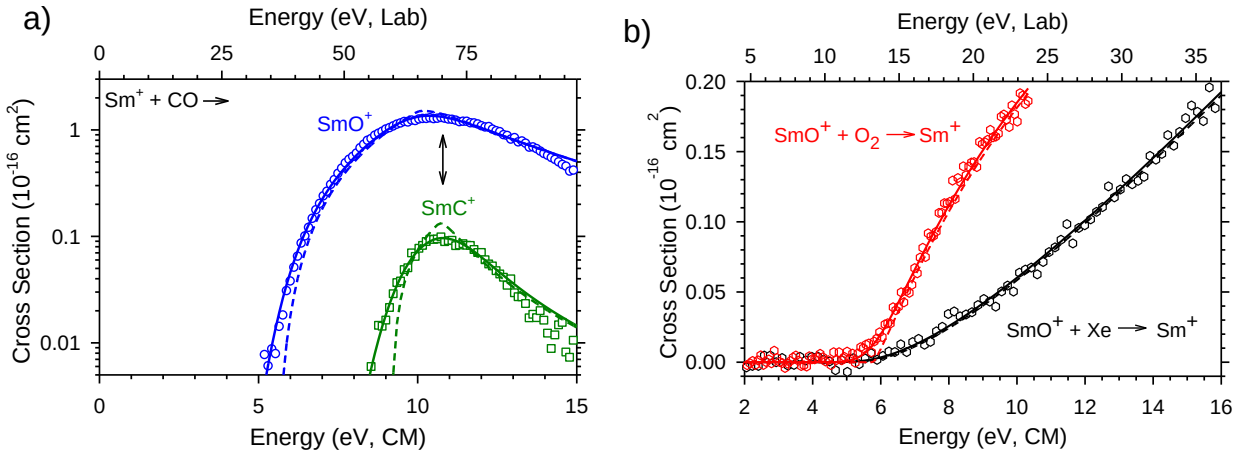

Fig. 2. Cross sections for reaction of Sm^+ with CO (part a) and SmO^+ + Xe and O_2 (part b) as a function of kinetic energy in the center-of-mass (lower x-axis) and laboratory (upper x-axis) frames (for Xe in part b). Dashed lines are models of the cross sections, and solid lines are the same models convoluted over the kinetic and internal energy distributions of the reactants. In part a, the arrow indicates the bond energy of the neutral reactant.

An important test of this value was also reported in our recent work.[2] The group of M. Heaven (Emory U.) measured IE(SmO) using resonantly enhanced two-photon ionization measurements (REMPI) and pulsed-field ionization zero kinetic energy (PFI-ZEKE) photoelectron spectroscopy. Their final result, 46318 ± 5 cm^{-1} (5.7427 ± 0.0006 eV), is 0.19 eV higher than the literature value of 5.55 ± 0.1 eV.[56] In previous work,[61-63] the IEs reported by Rauh and Ackermann[56,64] for ZrO, HfO, and TaO have also been found to be too low by even larger amounts. This systematic difference may occur because the population of excited states at the elevated temperatures used in these early experiments was not adequately accounted for. Combined with the literature value for $D_0(SmO) = 5.88 \pm 0.17$ eV and $IE(Sm) = 5.6437 \pm 0.0006$ eV, this refined IE(SmO) yields $D_0(SmO^+) = 5.78 \pm 0.17$ eV, in agreement with the GIBMS value. Conversely, combining these precise IEs with our value for $D_0(SmO^+)$ yields a refined neutral BDE of $D_0(SmO) = 5.83 \pm 0.07$ eV.

Finally, we return to the enthalpy for reaction 1. According to our measurements, the

SmO^+ bond energy is $5.72_5 \pm 0.07$ eV (weighted average of three values). Given this value and IE(Sm), the chemiionization reaction 1 is exothermic by 0.08 ± 0.07 eV, 0.25 eV lower than previously thought. Recent models of the MOSC test using this thermochemistry have nicely accounted for the observations made in the atmospheric tests. This result is also consistent with the original observations of both Fite and coworkers[65] and Dyke and coworkers[66] that the chemiionization process with samarium is observed with relatively small probabilities.

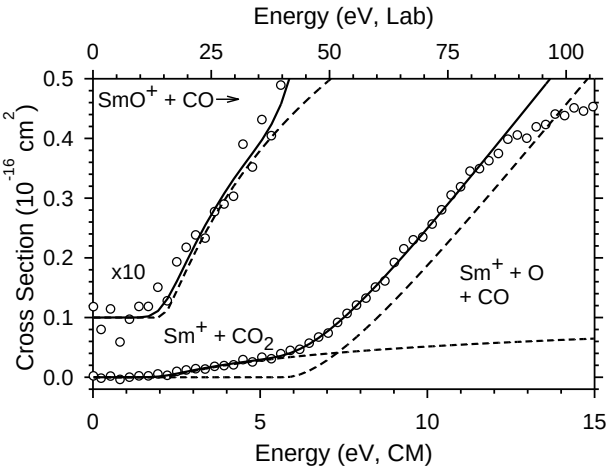

Fig. 3. Cross section for reaction of SmO^+ with CO as a function of kinetic energy in the center-of-mass (lower x-axis) and laboratory (upper x-axis) frames. Dashed lines are models of the cross sections, and the solid line is the sum of these models convoluted over the kinetic and internal energy distributions of the reactants.

As noted above, the observation of an appreciable barrier for the reactions with CO_2, OCS, and NO are interesting results that need to be explored more thoroughly, both experimentally and computationally. In the case of the CO_2 reaction, we have also examined the reverse reaction, $SmO^+ + CO \rightarrow Sm^+ + CO_2$, as shown in Figure 3. Comparison of this cross section with that for CID with Xe or O_2 (Figure 2b) shows that the sharp rise in the formation of Sm^+ at energies above ~6 eV can be attributed to CID. Therefore, the reactivity observed at low energies must correspond to formation of the CO_2 neutral product. This result unambiguously shows that there is a barrier in excess of the product asymptotes for both the forward and reverse reactions. The onset of this reverse reaction has a threshold energy consistent with the measured barrier height of the forward reaction, 1.84 ± 0.12 eV, combined with the calculated exothermicity of this reaction, $D_0(Sm^+\text{-}O) - D_0(OC\text{-}O) = 5.72_5 - 5.45_3$ eV $= 0.27 \pm 0.07$ eV, i.e., a reverse barrier height of 2.11 ± 0.14 eV, Figure 3.

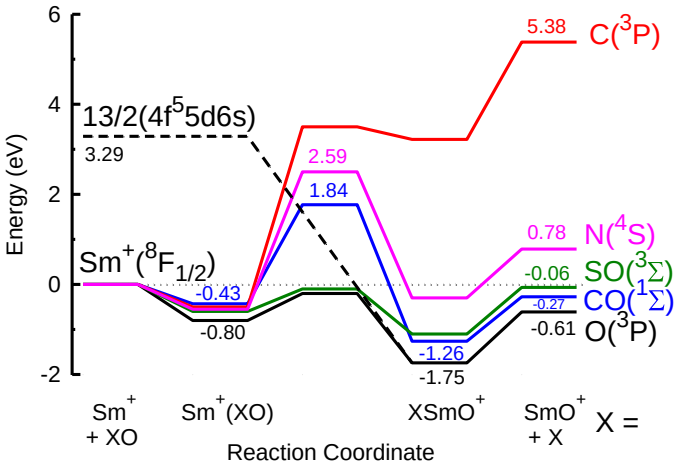

Fig. 4. Potential energy surfaces for oxidation of Sm^+ with O_2, CO_2, SO_2, NO, and CO. Small numbers indicate experimentally measured relative energies in eV. The location of the excited 13/2 state of Sm^+ is shown by the dashed line.

To further explore this potential energy surface, we have also examined the CID reactions of $OSm^+(CO)$ and $Sm^+(CO_2)$, species that are easily formed in the flow tube source by attaching the CO or CO_2 molecules to SmO^+ and Sm^+ using three-body association reactions. These experiments establish well depths of $D_0(OSm^+\text{–}CO) = 0.99 \pm 0.07$ eV and $D_0(Sm^+\text{–}CO_2) = 0.43 \pm 0.03$ eV. Thus, five points along the $Sm^+ + CO_2$ potential energy surface (reactants, products, two intermediates, and the barrier height) are experimentally established. These are shown in Figure 4 along with similar information on other oxidation reactions

studied here. Theoretical exploration of these potential energy surfaces, including consideration of spin-orbit effects, is now ongoing to complete our examination of these interesting systems. Our hypothesis for the origins of the barrier are also indicated in Figure 4. Namely, formation of a strong SmO^+ bond requires at least two electrons in the valence shell (non 4f).[67] The lowest energy state of Sm^+ that meets this requirement is a 13/2 state having a $4f^5 5d^1 6s^1$ configuration, 3.29 eV above the $^8F_{1/2}(4f^6 6s^1)$ ground state. The barriers are conjectured to be a result of the diabatic curve crossings between the surfaces evolving from these two states. An interesting question remains why the surfaces for the O_2 and SO_2 reactants have small barriers (lower than the reactants) whereas CO_2 and NO have large barriers, which may be related to the spin states of the neutral products, see Figure 4.

Another example of this type of study is shown in Figure 5. Here we show preliminary data for the gadolinium system in which GdO_2^+ is formed in the flow tube by addition of O_2, such that conceivably either GdO_2^+ (the dioxide) or $Gd^+(O_2)$ (the adduct) could be formed. The CID cross section with Xe clearly exhibits the formation of both $Gd^+ + O_2$ and $GdO^+ + O$, with the latter channel having both a low and high energy feature. (Although the low energy feature is noisy, its magnitude is decidedly above the baseline noise at the lowest energies below 0.3 eV.) What is not shown is that the magnitude (but not the kinetic energy dependence) of the Gd^+ and low-energy GdO^+ cross sections vary appreciably in magnitude (by over a factor of 10) as the source conditions are changed, whereas the higher energy GdO^+ feature remains static. This behavior combined with the relative thresholds indicates that both low energy features arise from dissociation of a minor amount of the $Gd^+(O_2)$ adduct, whereas the high energy GdO^+ feature comes from the GdO_2^+ dioxide, which dominates the population of these reactants. Note that the low-energy GdO^+ cross section is generally smaller than the Gd^+ cross section but does appear at slightly lower energies. This behavior is consistent with facile loss of O_2 from the $Gd^+(O_2)$ adduct whereas loss of O requires surmounting the insertion barrier leading to the GdO_2^+ dioxide and therefore is entropically disfavored. Analyses of these data along with the reactions $Gd^+ + O_2 \rightarrow GdO^+ + O$ (which like Sm^+ in Figure 1 occurs efficiently with no barrier) and $GdO^+ + O_2 \rightarrow GdO_2^+ + O$ (which is endothermic) means that we can measure the depths of the potential wells for both the adduct and the dioxide as well as the barrier height separating them (from the threshold for the low-energy GdO^+ feature in Figure 5). This latter analysis needs to include competition between the two pathways in order to achieve the most accurate information. Such a competitive analysis can be accomplished using statistical tools well-developed in our laboratory,[38] but requires knowledge of the molecular parameters of the products and the barrier along the potential energy surface. Again this points to have a more complete knowledge of the complete potential energy surface by examining this system computationally. A combined experimental/computational exploration of this potential energy surface should prove insightful.

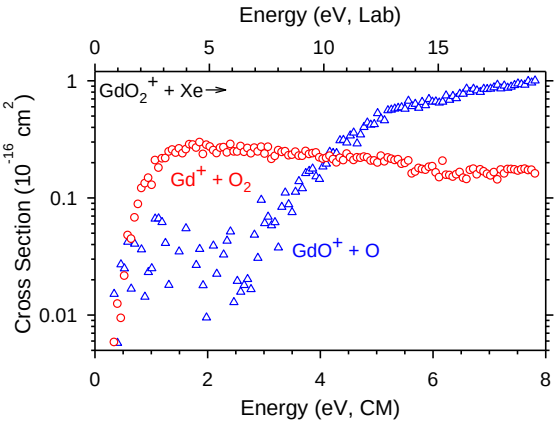

Fig. 5. Cross sections for reaction of GdO_2^+ + Xe as a function of kinetic energy in the center-of-mass (lower x-axis) and laboratory (upper x-axis) frames.

References

(1) Schofield, K., An Overlooked Series of Gas Phase Diatomic Metal Oxide Ions That Are Long-Lived. *J. Phys. Chem. A* **2006,** *110*, 6938-6947.

(2) Cox, R. M.; Kim, J.; Armentrout, P. B.; Bartlett, J.; VanGundy, R. A.; Heaven, M. C.; Ard, S. G.; Melko, J. J.; Shuman, N. S.; Viggiano, A. A., Evaluation of the Exothermicity of the Chemi-Ionization Reaction Sm + O $\rightarrow$ $SmO^+ + e^-$. *J. Chem. Phys.* **2015,** *142*, 134307.

(3) Ervin, K. M.; Armentrout, P. B., Translational Energy Dependence of $Ar^+ + XY \rightarrow ArX^+ + Y$ (XY = H_2, D_2, HD) from Thermal to 30 eV C.M. *J. Chem. Phys.* **1985,** *83*, 166-189.

(4) Armentrout, P. B.; Simons, J., Understanding Heterolytic Bond Cleavage. *J. Am. Chem. Soc.* **1992,** *114*, 8627-8633.

(5) Armentrout, P. B., Thermochemical Measurements by Guided Ion Beam Mass Spectrometry. In *Adv. Gas Phase Ion Chem.*, Adams, N.; Babcock, L. M., Eds. JAI Press: Greenwich, Connecticut, 1992; Vol. 1, pp 83-119.

(6) Armentrout, P. B., Not Just a Structural Tool: The Use of Guided Ion Beam Tandem Mass Spectrometry to Determine Thermochemistry. *J. Am. Soc. Mass Spectrom.* **2002,** *13*, 419-434.

(7) Schultz, R. H.; Armentrout, P. B., Reactions of N_4^+ with Rare Gases from Thermal to 10 eV C.M.: Collision-Induced Dissociation, Charge Transfer, and Ligand Exchange. *Int. J. Mass Spectrom. Ion Processes* **1991,** *107*, 29-48.

(8) Haynes, C. L.; Armentrout, P. B.; Perry, J. K.; Goddard, W. A., III, Experimental and Theoretical Studies of $Co(CH_4)_x^+$ with x = 1 - 4. *J. Phys. Chem.* **1995,** *99*, 6340-6346.

(9) Tjelta, B. L.; Armentrout, P. B., Gas-Phase Metal Ion Ligation: Collision-Induced Dissociation of $Fe(N_2)_x^+$ (x = 1 - 5) and $Fe(CH_2O)_x^+$ (x = 1 - 4). *J. Phys. Chem. A* **1997,** *101*, 2064-2073.

(10) Walter, D.; Sievers, M. R.; Armentrout, P. B., Alkali Ion Carbonyls: Sequential Bond Energies of $Li^+(CO)_x$ (x = 1 - 3), $Na^+(CO)_x$ (x = 1, 2), and $K^+(CO)$. *Int. J. Mass Spectrom.* **1998,** *173*, 93-106.

(11) Andersen, A.; Muntean, F.; Walter, D.; Rue, C.; Armentrout, P. B., Collision-Induced Dissociation and Theoretical Studies of Mg^+ Complexes with CO, CO_2, NH_3, CH_4, CH_3OH, and C_6H_6. *J. Phys. Chem. A* **2000,** *104*, 692-705.

(12) Armentrout, P. B., The Kinetic Energy Dependence of Ion-Molecule Reactions: Guided Ion Beams and Threshold Measurements. *Int. J. Mass Spectrom.* **2000,** *200*, 219-241.

(13) Tjelta, B. L.; Walter, D.; Armentrout, P. B., Determination of Weak Fe^+-L Bond Energies (L = Ar, Kr, Xe, N_2, CO_2) by Ligand Exchange Reactions and Collision-Induced Dissociation. *Int. J. Mass Spectrom.* **2001,** *204*, 7-21.

(14) Armentrout, P. B.; Kickel, B. L., Gas-Phase Thermochemistry of Transition Metal Ligand Systems: Reassessment of Values and Periodic Trends. In *Organometallic Ion Chemistry*, Freiser, B. S., Ed. Kluwer: Dordrecht, 1996; pp 1-45.

(15) Armentrout, P. B., Gas Phase Organometallic Chemistry. In *Topics in Organometallic Chemistry*, Brown, J. M.; Hofmann, P., Eds. Springer-Verlag: Berlin, 1999; Vol. 4, pp 1-45.

(16) Cox, R. M.; Armentrout, P. B.; de Jong, W. A., Activation of CH_4 by Th^+ as Studied by Guided Ion Beam Mass Spectrometry and Quantum Chemistry. *Inorg. Chem.* **2015**, in press.

(17) Kickel, B. L.; Armentrout, P. B., Guided Ion Beam Studies of the Reactions of Group 3 Metal Ions (Sc^+, Y^+, La^+, and Lu^+) with Silane. Electronic State Effects, Comparison to Reactions with Methane, and M^+-SiH_x (x = 0 - 3) Bond Energies. *J. Am. Chem. Soc.* **1995,** *117*, 4057-4070.

(18) Clemmer, D. E.; Chen, Y.-M.; Khan, F. A.; Armentrout, P. B., State-Specific Reactions of $Fe^+(A^6d, A^4f)$ with D_2O and Reactions of Feo^+ with D_2. *J. Phys. Chem.* **1994,** *98*, 6522-6529.

(19) Haynes, C. L.; Armentrout, P. B., Thermochemistry and Structures of $Coc_3h_6^+$: Metallacycle and Metal-Alkene Isomers. *Organomet.* **1994,** *13*, 3480-3490.

(20) Kickel, B. L.; Armentrout, P. B., Reactions of Fe^+, Co^+ and Ni^+ with Silane. Electronic State Effects and M^+-SiH_x (x = 0 - 3) Bond Energies. *J. Am. Chem. Soc.* **1995,** *117*, 764-773.

(21) Chen, Y.-M.; Elkind, J. L.; Armentrout, P. B., Reactions of Ru^+, Rh^+, Pd^+, and Ag^+ with H_2, HD and D_2. *J. Phys. Chem.* **1995,** *99*, 10438-10445.

(22) Sievers, M. R.; Chen, Y.-M.; Elkind, J. L.; Armentrout, P. B., Reactions of Y^+, Zr^+, Nb^+, and Mo^+ with H_2, HD, and D_2. *J. Phys. Chem.* **1996,** *100*, 54-62.

(23) Walter, D.; Armentrout, P. B., Sequential Bond Dissociation Energies of $M^+(NH_3)_x$ (x = 1 - 4) for M = Ti - Cu. *J. Am. Chem. Soc.* **1998,** *120*, 3176-3187.

(24) Armentrout, P. B.; Rodgers, M. T., An Absolute Sodium Cation Affinity Scale: Threshold Collision-Induced Dissociation Experiments and Ab Initio Theory. *J. Phys. Chem. A* **2000,** *104*, 2238-2247.

(25) Rodgers, M. T.; Armentrout, P. B., Noncovalent Metal-Ligand Bond Energies as Studied by Threshold Collision-Induced Dissociation. *Mass Spectrom. Rev.* **2000,** *19*, 215-247.

(26) Gerlich, D., Inhomogeneous rf Fields: A Versatile Tool for the Study of Processes with Slow Ions. *Adv. Chem. Phys.* **1992,** *82*, 1-176.

(27) Muntean, F.; Armentrout, P. B., Guided Ion Beam Study of Collision-Induced Dissociation Dynamics: Integral and Differential Cross Sections. *J. Chem. Phys.* **2001,** *115*, 1213-1228.

(28) Daly, N. R., Scintillation Type Mass Spectrometer Ion Detector. *Rev. Sci. Instrum.* **1960,** *31*, 264-267.

(29) Burley, J. D.; Ervin, K. M.; Armentrout, P. B., Translational Energy Dependence of $O^+(^4s)$ + $H_2(D_2, HD)$ –> $OH^+(OD^+)$ + H(D) from Thermal to 30 eV C.M. *Int. J. Mass Spectrom. Ion Processes* **1987,** *80*, 153-175.

(30) Gioumousis, G.; Stevenson, D. P., Reactions of Gaseous Molecule Ions with Gaseous Molecules. V. Theory. *J. Chem. Phys.* **1958,** *29*, 294-299.

(31) Robinson, P. J.; Holbrook, K. A., *Unimolecular Reactions*. Wiley Interscience: New York, 1972.

(32) Gilbert, R. G.; Smith, S. C., *Theory of Unimolecular and Recombination Reactions*. Blackwell Scientific: London, 1990.

(33) Schultz, R. H.; Crellin, K. C.; Armentrout, P. B., Sequential Bond Energies of $Fe(CO)_x^+$ (x = 1 - 5): Systematic Effects on Collision-Induced Dissociation Measurements. *J. Am. Chem. Soc.* **1991,** *113*, 8590-8601.

(34) Chantry, P. J., Doppler Broadening in Beam Experiments. *J. Chem. Phys.* **1971,** *55*, 2746-2759.

(35) Lifshitz, C.; Wu, R. L. C.; Tiernan, T. O.; Terwilliger, D. T., Negative Ion-Molecule Reactions of Ozone and Their Implications on the Thermochemistry of O_3^-. *J. Chem. Phys.* **1978,** *68*, 247-260.

(36) Khan, F. A.; Clemmer, D. E.; Schultz, R. H.; Armentrout, P. B., Sequential Bond Energies of $Cr(CO)_x^+$, x = 1 - 6. *J. Phys. Chem.* **1993,** *97*, 7978-7987.

(37) Rodgers, M. T.; Ervin, K. M.; Armentrout, P. B., Statistical Modeling of Collision-Induced Dissociation Thresholds. *J. Chem. Phys.* **1997,** *106*, 4499-4508.

(38) Rodgers, M. T.; Armentrout, P. B., Statistical Modeling of Competitive Threshold Collision-Induced Dissociation. *J. Chem. Phys.* **1998,** *109*, 1787-1800.

(39) Amicangelo, J. C.; Armentrout, P. B., Relative and Absolute Bond Dissociation Energies of Sodium Cation Complexes Determined Using Competitive Collision-Induced Dissociation Experiments. *Int. J. Mass Spectrom.* **2001,** *212*, 301-325.

(40) Muntean, F.; Armentrout, P. B., Modeling Kinetic Shifts for Tight Transition States in Threshold Collision-Induced Dissociation. Case Study: Phenol Cation. *J. Phys. Chem. B* **2002,** *106*, 8117-8124.

(41) Muntean, F.; Armentrout, P. B., Modeling Kinetic Shifts and Competition in Threshold Collision-Induced Dissociation. Case Study: *n*-Butylbenzene Cation Dissociation. *J. Phys. Chem. A* **2003,** *107*, 7413-7422.

(42) Muntean, F.; Heumann, L.; Armentrout, P. B., Modeling Kinetic Shifts in Threshold Collision-Induced Dissociation. Case Study: Dichlorobenzene Cation Dissociation. *J. Chem. Phys.* **2002,** *116*, 5593-5602.

(43) Koizumi, H.; Muntean, F.; Armentrout, P. B., Reaction of Cu^+ with Dimethoxyethane: Competition between Association and Multiple Dissociation Channels. *J. Chem. Phys.* **2004,** *120*, 756-766.

(44) Koizumi, H.; Armentrout, P. B., The Kinetic Energy Dependence of Association Reactions. A New Thermokinetic Method for Large Systems. *J. Chem. Phys.* **2003,** *119*, 12819-12829.

(45) Amicangelo, J. C.; Armentrout, P. B., Ligand Exchange Reactions of Sodium Cation Complexes Examined Using Guided Ion Beam Mass Spectrometry: Relative and Absolute Dissociation Free Energies and Entropies. *J. Phys. Chem. A* **2004,** *108*, 10698-10713.

(46) Armentrout, P. B., Statistical Modeling of Sequential Collision-Induced Dissociation Thresholds. *Journal of Chemical Physics* **2007,** *126*, 234302/234301-234302/234309.

(47) Hinton, C. S.; Citir, M.; Armentrout, P. B., Guided Ion-Beam and Theoretical Studies of the Reaction of Os^+ (^{6}d) with O_2: Adiabatic and Nonadiabatic Behavior. *Int. J. Mass Spectrom.* **2013,** *78*, 1157-1173.

(48) Ames, L. L.; Walsh, P. N.; White, D., Rare Earths. Iv. Dissociation Energies of the Gaseous Monoxides of the Rare Earths. *J. Phys. Chem. A* **1967,** *71*, 2707.

(49) Dickson, C. R.; Zare, R. N., Beam Gas Chemiluminescent Reactions of Eu and Sm with O_3, N_2O, NO_2, and F_2. *Chem. Phys.* **1975,** *7*, 361.

(50) Hildenbrand, D. L., Dissociation Energy of Samarium Monoxide and Its Relation to That of Europium Monoxide. *Chem. Phys. Lett.* **1977,** *48*, 340.

(51) Brewer, L.; Rosenblatt, G. M., Dissociation Energies and Free Energy Functions of Gaseous Monoxides. In *Adv. High Temp. Chem.*, Eyring, L., Ed. Academic: New York, 1969; Vol. 2, pp 1-83.

(52) Pedley, J. B.; Marshall, E. M., Thermochemical Data for Gaseous Monoxides. *J. Phys. Chem. Ref. Data* **1983,** *12*, 967-1031.

(53) Chandrasekharaiah, M. S.; Gingerich, K. A., In *Handbook on the Physics and Chemistry of Rare Earths*, Gschneidner, K. A.; Jr., L. E., Eds. Elsevier: Amsterdam, 1989.

(54) Lias, S. G.; Bartmess, J. E.; Liebman, J. F.; Holmes, J. L.; Levin, R. D.; Mallard, W. G., Gas-Phase Ion and Neutral Thermochemistry. *J. Phys. Chem. Ref. Data Suppl. 1* **1988,** *17*, 1.

(55) Konings, R. J. M.; Benes, O.; Kovacs, A.; Manara, D.; Sedmidubsky, D.; Gorokhov, L.; Iorish, V. S.; Yungman, V.; Shenyavskaya, E.; Osina, E., The Thermodynamic Properties of the F-Elements and Their Compounds. Part 2. The Lanthanide and Actinide Oxides. *J. Phys. Chem. Ref. Data* **2014,** *43*, 013101.

(56) Ackermann, R. J.; Rauh, E. G.; Thorn, R. J., The Thermodynamics of Ionization of Gaseous Oxides; the First Ionization Potentials of the Lanthanide Metals and Monoxides. *J. Chem. Phys.* **1976,** *65*, 1027-1031.

(57) Jaysekharan, T.; Razvi, M. A. N.; Bhale, G. L., Even-Parity Bound and Autoionizing Rydberg Series of the Samarium Atom. *J. Phys. B* **2000,** *33*, 3123-3136.

(58) Martin, W. C.; Zalubas, R.; Hagan, L., Atomic Energy Levels - the Rare Earth Elements. *Natl. Stand. Ref. Data Ser., Natl. Bur. Stand. (U.S.)* **1978,** *60*, 1.

(59) Koyanagi, G. K.; Bohme, D. K., Oxidation Reactions of Lanthanide Cations with N_2O and O_2: Periodicities in Reactivity. *J. Phys. Chem. A* **2001,** *105*, 8964-8968.

(60) Su, T.; Chesnavich, W. J., Parameterization of the Ion-Polar Molecule Collision Rate Constant by Trajectory Calculations. *J. Chem. Phys.* **1982,** *76*, 5183-5185.

(61) Sievers, M. R.; Chen, Y.-M.; Armentrout, P. B., Metal Oxide and Carbide Thermochemistry of Y^+, Zr^+, Nb^+, and Mo^+. *J. Chem. Phys.* **1996,** *105*, 6322-6333.

(62) Hinton, C. S.; Li, F.-X.; Armentrout, P. B., Reactions of Hf^+, Ta^+, and W^+ with O_2 and CO: Metal Carbide and Metal Oxide Cation Bond Energies. *Int. J. Mass Spectrom.* **2009,** *280*, 226-234.

(63) Hinton, C. S.; Citir, M.; Manard, M.; Armentrout, P. B., Collision-Induced Dissociation of Mo^+ and Mo_2^+ (M = Ta and W): Metal Oxide and Dioxide Cation Bond Energies. *Int. J. Mass Spectrom.* **2011,** *308*, 265-274.

(64) Rauh, E. G.; Ackermann, R. J., First Ionization Potentials of Some Refractory Oxide Vapors *J. Chem. Phys.* **1974,** *60*, 1396-1400.

(65) Fite, W. L.; Patterson, T. A.; Siegel, M. W. *Cross Sections for Thermal Reactions between Uranium Atoms and Atmospheric Species*; Air Force Geophysics Laboratory, Hanscom Air Force Base MA, Report No. AFGL-TR-77-0030, NTIS Access No. AD/A 038806: 1976; pp 1-88.

(66) Cockett, M. C. R.; Nyulaszi, L.; Veszpremi, T.; Wright, T. G.; Dyke, J. M., A Study of Some Gas-Phase Lanthanide Plus Oxidant Chemiionization Reactions with Chemielectron Spectroscopy. *J. Electron Spectros. Relat. Phenom.* **1991,** *57*, 373-397.

(67) Gibson, J. K., Role of Atomic Electronics in F-Element Bond Formation: Bond Energies of Lanthanide and Actinide Oxide Molecules. *J. Phys. Chem. A* **2003,** *107*, 7891-7899.